CLIMATOLOGY

Geologic evidence for an icehouse Earth before the Sturtian global glaciation

Scott A. MacLennan[1,2]*, Michael P. Eddy[3], Arthur J. Merschat[4], Akshay K. Mehra[1,5], Peter W. Crockford[1,6], Adam C. Maloof[1], C. Scott Southworth[4], Blair Schoene[1]

Snowball Earth episodes, times when the planet was covered in ice, represent the most extreme climate events in Earth's history. Yet, the mechanisms that drive their initiation remain poorly constrained. Current climate models require a cool Earth to enter a Snowball state. However, existing geologic evidence suggests that Earth had a stable, warm, and ice-free climate before the Neoproterozoic Sturtian global glaciation [ca. 717 million years (Ma) ago]. Here, we present eruption ages for three felsic volcanic units interbedded with glaciolacustrine sedimentary rocks from southwest Virginia, USA, that demonstrate that glacially influenced sedimentation occurred at tropical latitudes ca. 751 Ma ago. Our findings are the first geologic evidence of a cool climate teetering on the edge of global glaciation several million years before the Sturtian Snowball Earth.

INTRODUCTION

Glacial coverage is controlled by the global distribution of surface temperatures and the rate of temperature change with altitude (lapse rate). Today, these variables lead to a configuration where the snow line is at sea level near the poles and at high altitude in the tropics. Snowball Earth episodes represent a departure from this state, where the sea level snow line extends through the tropics. Potential causative mechanisms for Snowball initiation fall into two categories: (i) changes in the atmosphere's greenhouse gas budget (*1*–*3*) and (ii) changes in planetary albedo (*4*, *5*). Critical to testing, the viability of these models is the initial climate boundary condition.

Most initiation models assume a cold climate immediately before the first Neoproterozoic Snowball Earth [ca. 717 million years (Ma) ago], invoking tectonically controlled mechanisms such as increased planetary albedo related to the presence of a tropical supercontinent and elevated CO_2 sequestration through weathering of mafic rocks along convergent and divergent margins (*3*, *6*, *7*). However, this assumption is difficult to test because the only climate proxies currently available for the Neoproterozoic are geologic. Snowball Earth episodes, with evidence of equatorial sea ice, represent the only times during the Neoproterozoic where global climate is constrained. The Tonian Period (1000 to 717 Ma ago) preceding the first Neoproterozoic Snowball Earth has an apparent absence of glacially influenced sedimentary rocks and an abundance of platform carbonates and evaporites, consistent with an Earth that had a stable, ice-free climate. Rapid exit from such a climate state would require an extraordinarily powerful trigger because a warm ocean-atmosphere system has a substantial buffering effect on climate (*4*). The interpretation of a warm global climate before the onset of Snowball Earth episodes rests on the assumption that all Neoproterozoic glaciogenic sedimentary rocks belong to one of three globally correlative glacial episodes: the Sturtian [717–659 Ma ago (*8*–*11*)], the Marinoan [639–635 Ma ago (*12*, *13*)], or the Gaskiers [ca. 580 Ma ago (*14*)]. However, there are glaciogenic sedimentary rocks with poor age control or disputed stratigraphic correlations [e.g., (*15*)] that may predate the Sturtian, including the Kaigas Formation in Namibia (*16*, *17*), the Quruqtagh Group in northwest China (*18*), and the Konnarock Formation in Virginia, USA (*19*).

Konnarock Formation

To better characterize Earth's climate state before the Sturtian glaciation, we have constrained the depositional age of the Konnarock Formation by dating zircon crystals isolated from intercalated felsic volcanic rocks using isotope dilution–thermal ionization mass spectrometry (ID-TIMS) U-Pb geochronology. Our samples are from a structurally continuous sedimentary succession in southwest Virginia consisting of the Mount Rogers, Konnarock, and Unicoi Formations (Fig. 1A). The stratigraphy lies unconformably on 1.3– to 1.0–billion year gneiss related to the Grenville orogeny, implying an autochthonous relationship and that the sequence is not exotic to Laurentia (*19*, *20*). This stratigraphic relationship also implies that the paleomagnetic record from Laurentia may be used to constrain the depositional paleolatitude of the overlying Neoproterozoic sedimentary rocks. Multiple paleomagnetic studies robustly constrain eastern Laurentia (modern eastern and central United States) to low latitudes for most of the Tonian (*21*–*25*).

The Mount Rogers Formation comprises predominantly felsic volcanics and associated sedimentary rocks that were deposited ca. 755 Ma ago (*26*–*28*). The <1100-m-thick Konnarock Formation overlies the Mount Rogers Formation and consists of argillite, fine siliciclastics, and massive and stratified diamictite, with clasts up to boulder size (*19*, *20*). The limited outcrop area, relatively thick sedimentary sequence that includes debris flow deposits and massive to graded sandstones, and presumed association with bimodal volcanics in the Mount Rogers Formation suggest that the Konnarock Formation was deposited in a continental rift undergoing rapid subsidence (*29*). However, the rhythmic appearance of the argillites in the Konnarock Formation, the presence of outsize clasts of Grenville granite gneiss, early lithified frozen till fragments, and dropstones (Fig. 1B) support glacially influenced deposition within a lacustrine setting during rifting (*29*–*34*). The Unicoi Formation of the lower Chilhowee Group unconformably overlies the Konnarock Formation (*20*). On the basis of the lithological correlation of basaltic flows in

[1]Department of Geosciences, Princeton University, Princeton, NJ, USA. [2]Department of Earth and Environmental Sciences, University of Rochester, Rochester, NY, USA. [3]Department of Earth, Atmospheric, and Planetary Sciences, Purdue University, West Lafayette, IN, USA. [4]Florence Bascom Geoscience Center, United States Geological Survey, MS926A, Reston, VA, USA. [5]Department of Earth Sciences, Dartmouth College, Hanover, NH, USA. [6]Weizmann Institute of Science, Rehovot, Israel.
*Corresponding author. Email: sam7@alumni.princeton.edu

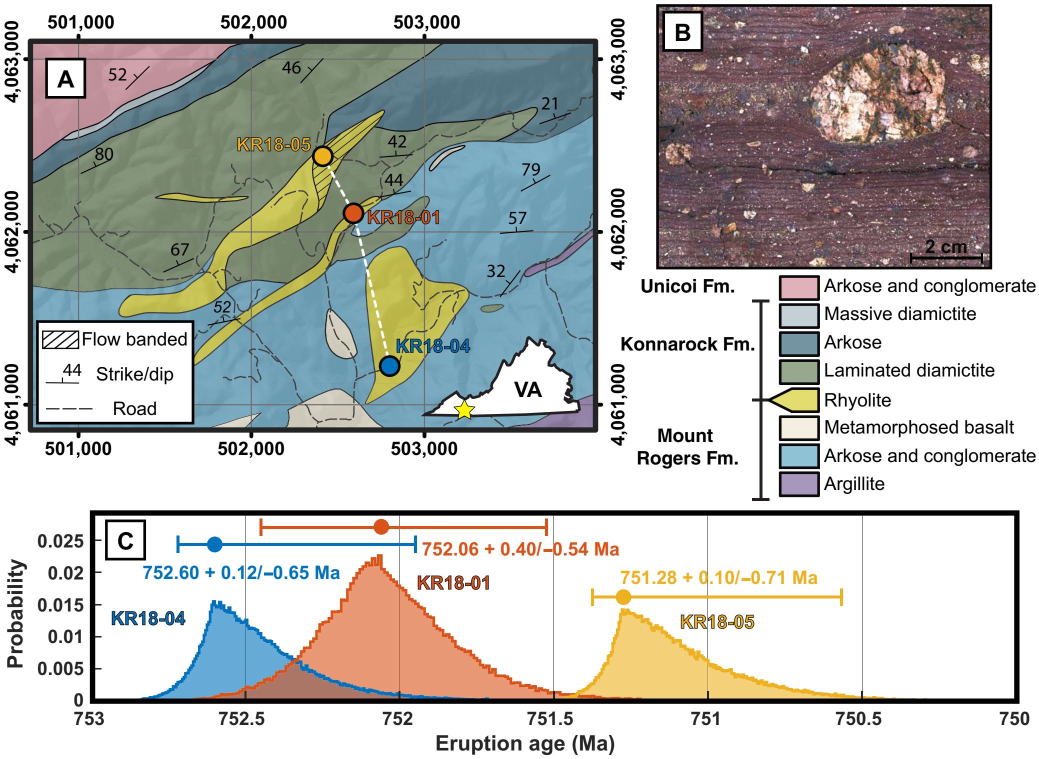

Fig. 1. Geological map of the study area and rhyolite eruption age estimates from within the Konnarock Formation. (**A**) Geological map of the study area with samples depicted as colored circles. Coordinates are in Universal Transverse Mercator zone 17N [World Geodetic System (WGS) 84]. A geological map placing the study area in a broader context is available in fig. S1. (**B**) Example of a coarse gravel-sized granite dropstone in laminated diamictite of the Konnarock Formation (Fm.) collected along strike west of the mapped area. (**C**) Bayesian eruption age probability distributions for the three dated rhyolite samples. Eruption age modes and 95% credible intervals are displayed. Photo credit: Scott MacLennan, Princeton University.

the Catoctin Formation, a maximum age of ca. 570 Ma ago has been assigned to the basal Chilhowee Group (*26*). Glaciolacustrine deposition as recorded by the Konnarock formation is therefore currently temporally constrained between the late Tonian and early Cambrian (ca. 750 to 570 Ma ago) (*19*, *20*, *28*).

Despite previous U-Pb geochronology from the Mount Rogers Formation (*26*, *27*), more precise age constraints for Konnarock Formation are unavailable because the unit has not been dated directly, and its depositional relationship to the underlying Mount Rogers Formation remains unresolved. The nature of the contact between these two formations has been interpreted to be conformable, unconformable, and structural (*19*, *20*, *28*, *35*).

The uppermost Mount Rogers Formation and lowermost Konnarock Formation contain several bodies of rhyolite that are up to ca. 2000 m wide and 300 m thick (*19*, *28*, *35*), which are appropriate for U-Pb zircon dating. Concordance with local strike and dip, along with the presence of flow banding and transitional volcaniclastic facies, provides evidence that these units are syndepositional. To further test this interpretation, we collected three rhyolite samples in stratigraphic order, spanning the contact between the uppermost Mount Rogers Formation (KR18-04 and KR18-01) and the overlying Konnarock Formation (KR18-05; Fig. 1) for U-Pb ID-TIMS zircon geochronology. Sample descriptions, isotopic data, and analytical methods are described in the Supplementary Materials. If the eruption ages for these rhyolites follow the law of superposition, then they can be used to assess the depositional relationship between the Mount Rogers and Konnarock Formations and the timing of glaciolacustrine sedimentation.

RESULTS

Zircons were separated from our rhyolite samples using traditional mineral separation techniques (see Materials and Methods). The zircons are predominantly clear and euhedral and frequently fragmented, likely during mineral separation. Pb loss is apparent in U-Pb concordia space for many grains, despite the use of the chemical abrasion technique (*36*). However, all three samples exhibit populations of zircon that are the same age within analytical uncertainty. We interpret these populations to represent pre- and syneruptive zircon growth and use them to estimate eruption ages using a Bayesian Markov Chain Monte Carlo technique (*37*). The resulting eruption ages are 752.60 + 0.12/−0.65 Ma ago for KR18-04, 752.06 + 0.40/−0.54 Ma ago for KR18-01, and 751.28 + 0.10/−0.71 Ma ago for KR18-05 (Fig. 1C; 95% credible interval, analytical uncertainties only) and satisfy the law of superposition. As a result, we interpret these rhyolites to be syndepositional flows that constrain the age of the sedimentary rocks around them.

DISCUSSION

Numerous paleomagnetic studies constrain Laurentia to low latitudes during the Tonian (*21*–*24*). In particular, recent geochronologic

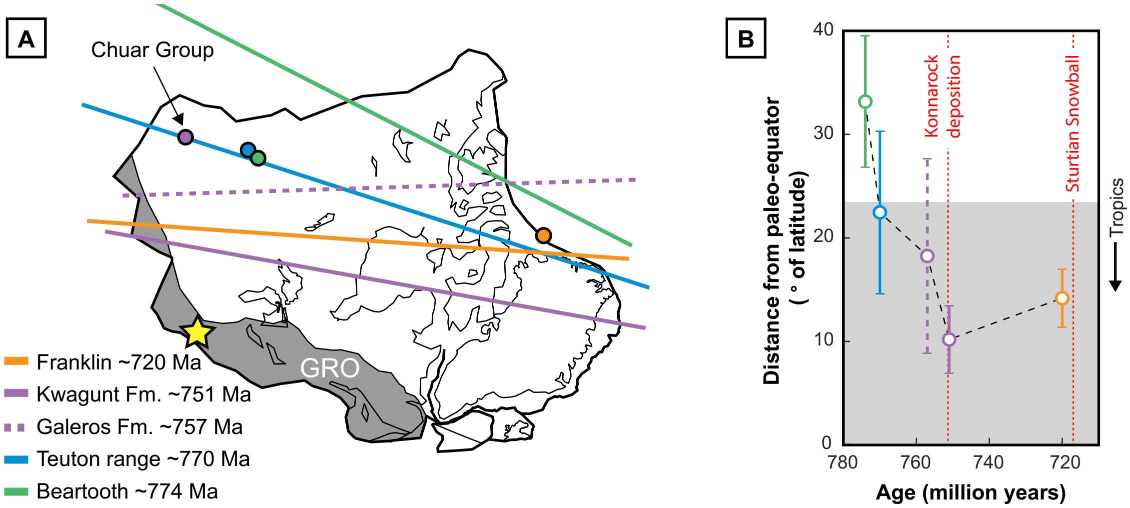

Fig. 2. Map of Laurentia with paleolatitudinal constraints on the Konnarock Formation. (**A**) Paleogeographic map of Laurentia (Mercator projection), with the location of the Konnarock Formation shown by the yellow star. The location of paleomagnetic sites (colored circles) and their paleo-equators (*21*–*25*) is depicted. Ages for paleomagnetic poles derived from the Kwagunt and Galeros Formations have been updated based on new geochronologic and paleomagnetic data (*25*, *38*). The extent of basement rocks involved in the Grenville orogeny (GRO) is shown in gray. (**B**) Latitudinal distance between the Konnarock Formation depositional area and available paleo-equators between 780 and 710 Ma ago. The timing of Konnarock Formation deposition and initiation of the Sturtian Snowball Earth are shown by dashed red lines.

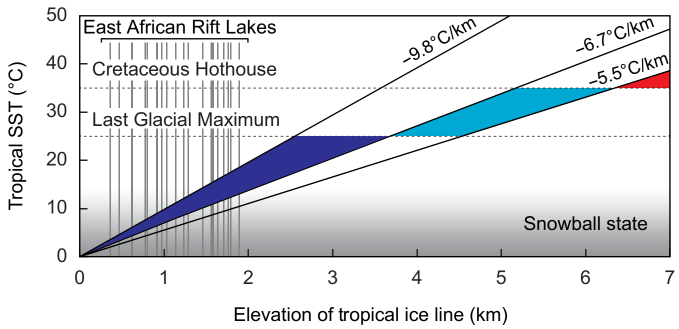

Fig. 3. Plot of potential paleo-altitudes of the Konnarock Formation and implied tropical SST. Relationship between tropical STT and altitude of the tropical snow line. Modern/LGM (*52*) and Cretaceous (*39*) SSTs are shown, along with the dry (9.8°C/km), LGM (6.7°C/km) (*41*), and humid (5.5°C/km) lapse rates. Red, light blue, and dark blue areas respectively correspond to the climate conditions needed for tropical ice during the Cretaceous, LGM, and a hypothetical colder climate. Tropical SST at Snowball initiation estimated using the average LGM (*52*) latitudinal temperature gradient as a lower bound. The elevation of major East African Rift lakes is shown by gray lines.

(*38*) and paleomagnetic (*25*) data from the Chuar Group in Arizona, USA, necessitate equatorial paleolatitudes for the modern eastern United States ca. 751 Ma ago (Fig. 2). Given the autochthonous contact between the Konnarock Formation and Laurentian basement, these data constrain the paleolatitude of these rocks to ca. 10°S during deposition. As a result, the presence of sample KR18-05 stratigraphically above laminated diamictite constrains tropical glaciolacustrine sedimentation to ca. 751 Ma ago, ~33 Ma before the start of the Sturtian glaciation (*8*, *10*).

The presence of tropical glaciers provides an important first-order constraint on Earth's climate before the Sturtian Snowball Earth. While the occurrence of glacially influenced rocks in the tropics suggests the possibility of Snowball Earth conditions, numerous observations of shallow water carbonate deposition within tropical latitudes ca. 751 Ma ago [e.g., (*9*)] preclude global glaciation. Nevertheless, the implications of tropical glaciers can be explored by examining the relationship between tropical snow line altitude and sea surface temperature (SST) for different climate states (Fig. 3). A tropical SST of ca. 35°C and a shallow lapse rate, similar to the ice-free Cretaceous (ca. 100 Ma ago) (*39*), would require deposition of the Konnarock Formation at altitudes >6 km. It is unlikely that rocks deposited at such high altitudes would be preserved in the geologic record. Furthermore, Laurentia was undergoing extension ca. 751 Ma ago, precluding the possibility of Himalaya-like mountains in this area. Rather, the failed rift setting recorded by the Mount Rogers and Konnarock Formations is suggestive of topography similar to the modern East African Rift (*29*, *40*). A steeper lapse rate (*41*) and a lower SST, similar to the Last Glacial Maximum (LGM), result in a tropical snow line altitude at ca. 3.5 to 4 km (Fig. 3) (*42*). Even colder conditions would lower the snow line until eventually runaway ice albedo feedback leads to Snowball initiation (Fig. 3). Snow line elevations of 1 to 3.5 km under these colder conditions are similar to the altitudes of modern lakes in the East African rift and may provide an analog for the depositional setting of the Konnarock Formation.

We suggest that the most parsimonious explanation for the evidence of tropical glaciation preserved in the Konnarock Formation is deposition in a glacial lake at an altitude of 1 to 3.5 km in a global climate that was as cold as—or colder than—the LGM. This observation provides the first geological constraint on climate during the Tonian and definitively invalidates any climate models for this period where average global temperatures are too high to support low-latitude glaciers. Whether the Konnarock Formation represents the background climate or a short-term glacial event is ambiguous. However, a temporally correlative change in marine $^{87}Sr/^{86}Sr$ toward less radiogenic values (*3*) is interpreted to reflect CO_2 sequestration through weathering of mafic rock (*7*) and supports the former. A prolonged period of cold conditions in the late Tonian is consistent with a global climate governed by relatively slow tectonic processes that was primed for global glaciation. If true, then models describing Snowball Earth initiation are incomplete without understanding the longer-term forcing that led to this climate boundary condition.

MATERIALS AND METHODS

Rhyolite samples were cut into small chips before being disaggregated using short runs in a SPEX 8530 ring and puck mill. The resulting material was sieved to <500 μm and panned to obtain a rough density separation. Following panning, magnetic minerals were removed with a hand magnet and repeated runs on a Frantz isodynamic magnetic separator. A pure zircon separate was then hand-picked from the resulting heavy, nonmagnetic fraction from each sample.

Zircons were dated at Princeton University using a modified version of chemical abrasion–ID-TIMS (*36*). Zircons were first annealed at 900°C and 1 atmosphere for 60 hours. Subsequently, individual zircons were loaded into Teflon perfluoroalkoxy alkane microcapsules with 100 to 125 μl of 29 M hydrofluoric acid (HF) and 25 μl of 30% HNO_3. The microcapsules were then loaded into a Parr dissolution vessel and held at 215°C for 12 to 14 hours. The resulting solutions were then discarded, and each individual zircon was repeatedly rinsed in 29 M HF, H_2O, and 6 N HCl. After rinsing, approximately ~0.006 g of EARTHTIME ^{202}Pb-^{205}Pb-^{233}U-^{235}U isotopic tracer (*43*, *44*) and 75 to 100 μl of 29 M HF were added to each microcapsule. The microcapsules were then reloaded into a Parr dissolution vessel and held at 215°C for 60 hours for total digestion. The solutions were then dried down and dissolved in 6 N HCl at 180°C for ~12 hours to convert the samples to chloride form. Uranium and Pb were purified from the dissolved sample with AG-1 X8 200- to 400-mesh anion exchange resin using methods modified from (*45*). Samples were loaded onto 50 μl of anion exchange columns in 50 to 75 μl of 3 N HCl and rinsed dropwise to remove trace elements. Then, Pb and U were eluted using 200 μl of 6 N HCl and 250 μl of H_2O, respectively. Samples were dried down with a microdrop of 0.05 M H_3PO_4 before analysis via TIMS.

All isotopic measurements were made on the IsotopX PhoeniX-62 TIMS at Princeton University. Lead was run as a metal and measured by peak hopping on a Daly photomultiplier. Uranium was analyzed as UO_2 and was measured statically on a series of faraday cups. Measured ratios were corrected assuming an $^{18}O/^{16}O$ of 0.00205 ± 0.00004 (2σ), corresponding to the modern atmospheric value (*46*). Corrections for mass-dependent fractionation were performed using the known ratios of $^{202}Pb/^{205}Pb$ and $^{233}U/^{235}U$ in the ET2535 isotopic tracer and assuming a $^{238}U/^{235}U$ of 137.818 ± 0.045 (2σ), which represents the mean value of $^{238}U/^{235}U$ measured in natural zircon (*47*). Corrections for Pb fractionation were performed cycle by cycle. However, the correction for U fractionation was performed using the mean $^{233}U/^{235}U$ for the analysis. Daly photomultiplier dead time for Pb was monitored by running the NBS981 and NBS982 Pb isotopic standards over the range 1000 counts per second to 2.5 Mcps over the course of the study.

A correction for common Pb (Pbc) was performed by assuming that all Pbc is from laboratory contamination and using the measured ^{204}Pb and a laboratory Pbc isotopic composition to subtract the appropriate mass of Pbc from each analysis.

A correction for initial secular disequilibrium in the ^{238}U-^{206}Pb system due to the exclusion of Th during zircon crystallization [e.g., (*48*)] was made for each analysis using a ratio of zircon/melt partition coefficients (f_{ThU}) of 0.23 to estimate the $[Th/U]_{Magma}$. These partition coefficients were empirically determined from measurements of glass and coexisting zircon rims or surfaces in a transitional tholeiitic-alkalic rhyolite erupted in Iceland [sample IETR in (*49*)]. Our estimated $[Th/U]_{Magma}$ values (5.78 to 3.48) are consistent with the composition of silicic magmas erupted in rift settings (*50*, *51*). Regardless, the effect of this correction is negligible (<100,000 years) for the dates reported in this study.

SUPPLEMENTARY MATERIALS

Supplementary material for this article is available at http://advances.sciencemag.org/cgi/content/full/6/24/eaay6647/DC1

REFERENCES AND NOTES

1. D. P. Schrag, R. A. Berner, P. F. Hoffman, G. P. Halverson, On the initiation of a Snowball Earth. *Geochem. Geophys. Geosyst.* **3**, 1–21 (2002).
2. E. Tziperman, I. Halevy, D. T. Johnston, A. H. Knoll, D. P. Schrag, Biologically induced initiation of Neoproterozoic snowball-Earth events. *Proc. Natl. Acad. Sci. U.S.A.* **108**, 15091–15096 (2011).
3. G. M. Cox, G. P. Halverson, R. K. Stevenson, M. Vokaty, A. Poirier, M. Kunzmann, Z.-X. Li, S. W. Denyszyn, J. V. Strauss, F. A. Macdonald, Continental flood basalt weathering as a trigger for Neoproterozoic Snowball Earth. *Earth Planet. Sci. Lett.* **446**, 89–99 (2016).
4. J. Bendtsen, C. J. Bjerrum, Vulnerability of climate on Earth to sudden changes in insolation. *Geophys. Res. Lett.* **29**, 1–4 (2002).
5. F. A. Macdonald, R. Wordsworth, Initiation of Snowball Earth with volcanic sulfur aerosol emissions. *Geophys. Res. Lett.* **44**, 1938–1946 (2017).
6. Y. Goddéris, Y. Donnadieu, A. Nédélec, B. Dupré, C. Dessert, A. Grard, G. Ramstein, L. M. François, The Sturtian "snowball" glaciation: Fire and ice. *Earth Planet. Sci. Lett.* **211**, 1–12 (2003).
7. Y. Goddéris, Y. Donnadieu, C. Dessert, B. Dupré, F. Fluteau, L. M. François, J. Meert, A. Nédélec, G. Ramstein, Coupled modeling of global carbon cycle and climate in the Neoproterozoic: Links between Rodinia breakup and major glaciations. *Compt. Rendus Geosci.* **339**, 212–222 (2007).
8. F. A. Macdonald, M. D. Schmitz, J. L. Crowley, C. F. Roots, D. S. Jones, A. C. Maloof, J. V. Strauss, P. A. Cohen, D. T. Johnston, D. P. Schrag, Calibrating the Cryogenian. *Science* **327**, 1241–1243 (2010).
9. A. D. Rooney, J. V. Strauss, A. D. Brandon, F. A. Macdonald, A Cryogenian chronology: Two long-lasting synchronous neoproterozoic glaciations. *Geology* **43**, 459–462 (2015).
10. S. A. MacLennan, Y. Park, N. Swanson-Hysell, A. Maloof, B. Schoene, M. Gebreslassie, E. Antilla, T. Tesema, M. Alene, B. Haileab, The arc of the Snowball: U-Pb dates constrain the Islay anomaly and the initiation of the Sturtian glaciation. *Geology* **46**, 539–542 (2018).
11. G. M. Cox, V. Isakson, P. F. Hoffman, T. M. Gernon, M. D. Schmitz, S. Shahin, A. S. Collins, W. Preiss, M. L. Blades, R. N. Mitchell, A. Nordsvan, South Australian U-Pb zircon (CA-ID-TIMS) age supports globally synchronous Sturtian deglaciation. *Precambrian Res.* **315**, 257–263 (2018).
12. K.-H. Hoffmann, D. J. Condon, S. A. Bowring, J. L. Crowley, U-Pb zircon date from the Neoproterozoic Ghaub Formation Namibia: Constraints on Marinoan glaciation. *Geology* **32**, 817–820 (2004).
13. A. R. Prave, D. J. Condon, K. H. Hoffmann, S. Tapster, A. E. Fallick, Duration and nature of the end-Cryogenian (Marinoan) glaciation. *Geology* **44**, 631–634 (2016).
14. J. P. Pu, S. A. Bowring, J. Ramezani, P. Myrow, T. D. Raub, E. Landing, A. Mills, E. Hodgin, F. A. Macdonald, Dodging snowballs: Geochronology of the Gaskiers glaciation and the first appearance of the Ediacaran biota. *Geology* **44**, 955–958 (2016).
15. F. A. Macdonald, J. V. Strauss, C. V. Rose, F. Ö. Ő. Dudás, D. P. Schrag, Stratigraphy of the Port Nolloth Group of Namibia and South Africa and implications for the age of Neoproterozoic iron formations. *Am. J. Sci.* **310**, 862–888 (2010).
16. H. E. Frimmel, U. S. Klötzli, P. R. Siegfried, New Pb-Pb single zircon age constraints on the timing of Neoproterozoic glaciation and continental break-up in Namibia. *J. Geol.* **104**, 459–469 (1996).
17. H. E. Frimmel, The Kaigas and Numees formations, Port Nolloth Group, in South Africa and Namibia. *Geol. Soc. Lond. Mem.* **36**, 223–231 (2011).
18. B. Xu, S. Xiao, H. Zou, Y. Chen, Z.-X. Li, B. Song, D. Liu, C. Zhou, X. Yuan, SHRIMP zircon U–Pb age constraints on Neoproterozoic Quruqtagh diamictites in NW China. *Precambrian Res.* **168**, 247–258 (2009).
19. A. J. Merschat, S. Southworth, E. McClellan, R. P. Tollo, D. W. Rankin, S. Hooper, S. Bauer, Key structural and stratigraphic relationships from the northeast end of the Mountain City window and the Mount Rogers area, Virginia–North Carolina–Tennessee, in *Elevating Geoscience in the Southeastern United States: New Ideas about Old Terranes*, C. M. Bailey, L. V. Coiner, Eds. (Geological Society of America, 2014) vol. 35, pp. 63–101.
20. D. W. Rankin, *The Volcanogenic Mount Rogers Formation and the Overlying Glaciogenic Konnarock Formation; Two Late Proterozoic Units in Southwestern Virginia* (USGPO; U.S. Geological Survey, Map Distribution, 1993).

21. J. K. Park, D. K. Norris, A. Larochelle, Paleomagnetism and the origin of the Mackenzie Arc of northwestern Canada. *Can. J. Earth Sci.* **26**, 2194–2203 (1989).
22. S. S. Harlan, J. W. Geissman, L. W. Snee, *Paleomagnetic and ^{40}Ar/^{39}Ar Geochronologic Data from Late Proterozoic Mafic Dikes and Sills, Montana and Wyoming* (U.S. Government Printing Office, 1997).
23. A. B. Weil, J. W. Geissman, R. Van der Voo, Paleomagnetism of the neoproterozoic chuar group, grand canyon supergroup, arizona: Implications for laurentia's neoproterozoic APWP and rodinia break-up. *Precambrian Res.* **129**, 71–92 (2004).
24. S. W. Denyszyn, H. C. Halls, D. W. Davis, D. A. D. Evans, Paleomagnetism and U–Pb geochronology of Franklin dykes in High Arctic Canada and Greenland: A revised age and paleomagnetic pole constraining block rotations in the Nares Strait region. *Can. J. Earth Sci.* **46**, 689–705 (2009).
25. A. Eyster, B. P. Weiss, K. Karlstrom, F. A. Macdonald, Paleomagnetism of the Chuar Group and evaluation of the late Tonian Laurentian apparent polar wander path with implications for the makeup and breakup of Rodinia. *Geol. Soc. Am. Bull.* **132**, 710–738 (2019).
26. J. N. Aleinikoff, R. E. Zartman, M. Walter, D. W. Rankin, P. T. Lyttle, W. C. Burton, U-Pb ages of metarhyolites of the Catoctin and Mount Rogers Formations, central and southern Appalachians: Evidence for two pulses of Iapetan rifting. *Am. J. Sci.* **295**, 428–454 (1995).
27. R. Tollo, J. N. Aleinikoff, R. Mundil, C. Scott Southworth, M. A. Cosca, D. W. Rankin, A. E. Rubin, A. E. Kentner, C. A. Parendo, M. S. Ray, in *From the Blue Ridge to the Coastal Plain; Field Excursions in the Southeastern United States* (Geological Society of America, 2012), vol. 29.
28. A. J. Merschat, S. Southworth, C. S. Holm-Denoma, R. J. McAleer, "Geology of the Mount Rogers area, revisited: Evidence of Neoproterozoic Continental Rifting, Glaciation, and the Opening and Closing of the Iapetus Ocean, Blue Ridge, VA–NC–TN" in *Geology of the Mount Rogers area, revisited, Blue Ridge, VA–NC–TN: Carolina Geological Society Annual Field Trip Guidebook*, A. J. Merschat, Ed. (Carolina Geological Society, 2016), pp. 3–28.
29. J. M. G. Miller, The Neoproterozoic Konnarock Formation, Southwestern Virginia, USA: Glaciolacustrine Facies in a Continental Rift, in *Earth's Glacial Record*, M. Deynoux, J. M. G. Miller, E. W. Domack, N. Eyles, I. Fairchild, G. M. Young, Eds. (Cambridge Univ. Press, 1994), pp. 47–59.
30. D. W. Rankin, *Guide to the Geology of the Mt. Rogers Area, Virginia, North Carolina and Tennessee: Carolina Geological Society, October 14–15, 1967, Field Trip Guidebook* (Carolina Geological Society, 1967).
31. D. W. Rankin, T. W. Stern, J. C. Reed, M. F. Newell, Zircon ages of felsic volcanic rocks in the upper Precambrian of the Blue Ridge, Appalachian Mountains. *Science* **166**, 741–744 (1969).
32. D. W. Rankin, Stratigraphy and structure of Precambrian rocks in northwestern North Carolina, in *Studies of Appalachian Geology: Central And Southern* (Interscience, 1970), pp. 227–245.
33. K. M. Blondeau, thesis, Louisiana State University (1975).
34. F. L. Schwab, Depositional environments, provenance, and tectonic framework; upper part of the late Precambrian Mount Rogers Formation, Blue Ridge Province, southwestern Virginia. *J. Sediment. Res.* **46**, 3–13 (1976).
35. D. W. Rankin, G. H. Espenshade, R. B. Neumann, *Geologic Map of the West Half of the Winston-Salem Quadrangle, North Carolina, Virginia, and Tennessee* (U.S. Geological Survey, 1972).
36. J. M. Mattinson, Zircon U–Pb chemical abrasion ("CA-TIMS") method: Combined annealing and multi-step partial dissolution analysis for improved precision and accuracy of zircon ages. *Chem. Geol.* **220**, 47–66 (2005).
37. C. B. Keller, B. Schoene, K. M. Samperton, A stochastic sampling approach to zircon eruption age interpretation. *Geochem. Perspect. Lett.* **8**, 31–35 (2018).
38. A. D. Rooney, J. Austermann, E. F. Smith, Y. Li, D. Selby, C. M. Dehler, M. D. Schmitz, K. E. Karlstrom, F. A. Macdonald, Coupled Re-Os and U-Pb geochronology of the Tonian Chuar Group, Grand Canyon. *GSA Bull.* **130**, 1085–1098 (2018).
39. C. L. O'Brien, S. A. Robinson, R. D. Pancost, J. S. S. Damsté, S. Schouten, D. J. Lunt, H. Alsenz, A. Bornemann, C. Bottini, S. C. Brassell, A. Farnsworth, A. Forster, B. T. Huber, G. N. Inglis, H. C. Jenkyns, C. Linnert, K. Littler, P. Markwick, A. McAnena, J. Mutterlose, B. D. A. Naafs, W. Püttmann, A. Sluijs, N. A. G. M. van Helmond, J. Vellekoop, T. Wagner, N. E. Wrobel, Cretaceous sea-surface temperature evolution: Constraints from TEX86 and planktonic foraminiferal oxygen isotopes. *Earth Sci. Rev.* **172**, 224–247 (2017).
40. W. A. Thomas, The Appalachian-Ouachita rifted margin of southeastern North America. *Geol. Soc. Am. Bull.* **103**, 415–431 (1991).
41. S. E. Loomis, J. M. Russell, D. Verschuren, C. Morrill, G. De Cort, J. S. Sinninghe Damsté, D. Olago, H. Eggermont, F. A. Street-Perrott, M. A. Kelly, The tropical lapse rate steepened during the Last Glacial Maximum. *Sci. Adv.* **3**, e1600815 (2017).
42. B. G. Mark, S. P. Harrison, A. Spessa, M. New, D. J. A. Evans, K. F. Helmens, Tropical snowline changes at the last glacial maximum: A global assessment. *Quat. Int.* **138**, 168–201 (2005).
43. D. J. Condon, B. Schoene, N. M. McLean, S. A. Bowring, R. R. Parrish, Metrology and traceability of U–Pb isotope dilution geochronology (EARTHTIME Tracer Calibration Part I). *Geochim. Cosmochim. Acta* **164**, 464–480 (2015).
44. N. M. McLean, D. J. Condon, B. Schoene, S. A. Bowring, Evaluating uncertainties in the calibration of isotopic reference materials and multi-element isotopic tracers (EARTHTIME Tracer Calibration Part II). *Geochim. Cosmochim. Acta* **164**, 481–501 (2015).
45. T. E. Krogh, A low-contamination method for hydrothermal decomposition of zircon and extraction of U and Pb for isotopic age determinations. *Geochim. Cosmochim. Acta* **37**, 485–494 (1973).
46. A. O. Nier, A redetermination of the relative abundances of the isotopes of carbon, nitrogen, oxygen, argon, and potassium. *Phys. Rev.* **77**, 789–793 (1950).
47. J. Hiess, D. J. Condon, N. McLean, S. R. Noble, ^{238}U/^{235}U systematics in terrestrial uranium-bearing minerals. *Science* **335**, 1610–1614 (2012).
48. U. Schärer, The effect of initial ^{230}Th disequilibrium on young U-Pb ages: The Makalu case, Himalaya. *Earth Planet. Sci. Lett.* **67**, 191–204 (1984).
49. L. L. Claiborne, C. F. Miller, G. A. R. Gualda, T. L. Carley, A. K. Covey, J. L. Wooden, M. A. Fleming, Zircon as magma monitor: Robust, temperature-dependent partition coefficients from glass and zircon surface and rim measurements from natural systems, in *Microstructural Geochronology: Planetary Records Down to Atom Scale* (American Geophysical Union, 2018), pp. 1–33.
50. C. B. Keller, B. Schoene, M. Barboni, K. M. Samperton, J. M. Husson, Volcanic–plutonic parity and the differentiation of the continental crust. *Nature* **523**, 301–307 (2015).
51. B. Schoene, M. P. Eddy, K. M. Samperton, C. B. Keller, G. Keller, T. Adatte, S. F. R. Khadri, U-Pb constraints on pulsed eruption of the Deccan Traps across the end-Cretaceous mass extinction. *Science* **363**, 862–866 (2019).
52. Members of the MARGO Project, Constraints on the magnitude and patterns of ocean cooling at the Last Glacial Maximum. *Nat. Geosci.* **2**, 127–132 (2009).
53. S. Southworth, J. N. Aleinikoff, R. P. Tollo, C. M. Bailey, W. C. Burton, P. C. Hackley, C. Mark Fanning, *From Rodinia to Pangea: The Lithotectonic Record of the Appalachian Region* (Geological Society of America, 2010).
54. R. L. Rexroad, thesis, Louisiana State University (1978).
55. J. F. Bowring, N. M. McLean, S. A. Bowring, Engineering cyber infrastructure for U-Pb geochronology: Tripoli and U-Pb_Redux. *Geochem. Geophys. Geosyst.* **12**, Q0AA19 (2011).
56. N. M. McLean, J. F. Bowring, S. A. Bowring, An algorithm for U-Pb isotope dilution data reduction and uncertainty propagation. *Geochem. Geophys. Geosyst.* **12**, Q0AA18 (2011).
57. A. H. Jaffey, K. F. Flynn, L. E. Glendenin, W. C. Bentley, A. M. Essling, Precision measurement of half-lives and specific activities of ^{235}U and ^{238}U. *Phys. Rev.* **C4**, 1889–1906 (1971).
58. I. Wendt, C. Carl, The statistical distribution of the mean squared weighted deviation. *Chem. Geol.* **86**, 275–285 (1991).
59. K. E. Karlstrom, S. A. Bowring, C. M. Dehler, A. H. Knoll, S. M. Porter, D. J. Des Marais, A. B. Weil, Z. D. Sharp, J. W. Geissman, M. B. Elrick, J. M. Timmons, L. J. Crossey, K. L. Davidek, Chuar Group of the Grand Canyon: Record of breakup of Rodinia, associated change in the global carbon cycle, and ecosystem expansion by 740 Ma. *Geology* **28**, 619–622 (2000).
60. M. I. Budyko, The effect of solar radiation variations on the climate of the Earth. *Tellus* **21**, 611–619 (1969).
61. W. D. Sellers, A global climatic model based on the energy balance of the earth-atmosphere system. *J. Appl. Meteorol.* **8**, 392–400 (1969).
62. M. Huber, A hotter greenhouse? *Science* **321**, 353–354 (2008).
63. L. Zhang, W. W. Hay, C. Wang, X. Gu, The evolution of latitudinal temperature gradients from the latest Cretaceous through the Present. *Earth Sci. Rev.* **189**, 147–158 (2019).

Acknowledgments: We thank N. Jeevanjee and G. Vecchi for helpful discussions that improved the manuscript. C. Bentley is thanked for inspiring our research in the Appalachians. S. Burgess and four anonymous reviewers are thanked for thorough reviews that improved the manuscript. Any use of trade, firm, or product names is for descriptive purposes only and does not imply endorsement by the U.S. government. **Funding:** This work was supported by the Scott Fund of the Department of Geosciences, Princeton University. The National Cooperative Geologic Mapping Program supported the field work of A.J.M and C.S.S. **Author contributions:** Conceptualization: M.P.E. and S.A.M. Investigation: S.A.M. and M.P.E. Geologic mapping: A.J.M. and C.S.S. Formal analysis: A.K.M. and S.A.M. Writing (original draft): S.A.M., M.P.E., A.K.M., and P.W.C. Writing (review and editing): A.C.M., A.J.M., B.S., and C.S.S. **Competing interests:** The authors declare that they have no competing interests. **Data and materials availability:** All data needed to evaluate the conclusions in the paper are present in the paper and/or the Supplementary Materials. Additional data related to this paper may be requested from the authors.

Submitted 8 July 2019
Accepted 17 April 2020
Published 10 June 2020
10.1126/sciadv.aay6647

Citation: S. A. MacLennan, M. P. Eddy, A. J. Merschat, A. K. Mehra, P. W. Crockford, A. C. Maloof, C. S. Southworth, B. Schoene, Geologic evidence for an icehouse Earth before the Sturtian global glaciation. *Sci. Adv.* **6**, eaay6647 (2020).